Received: 5 June 2020 | Revised: 4 November 2020 | Accepted: 7 December 2020

DOI: 10.1002/2050-7038.12763

RESEARCH ARTICLE

WILEY

A hybrid method for harmonic state estimation in partially observable systems

Gustavo G. Santos[1] | **Thales L. Oliveira**[2] | **José Carlos Oliveira**[3] | **José Carlos M. Vieira**[1]

[1]Department of Electrical and Computer Engineering, São Carlos School of Engineering, University of São Paulo, São Carlos, Brazil

[2]Federal Institute of Education Science and Technology of Goiás, Itumbiara Campus, Itumbiara, Brazil

[3]Faculty of Electrical Engineering, Universidade Federal de Uberlândia, Uberlândia, Brazil

Correspondence
Gustavo G. Santos, Department of Electrical and Computer Engineering, São Carlos School of Engineering, University of São Paulo, São Carlos, SP, 13566-590, Brazil.
Email: g.gustavo.santos@usp.br

Funding information
Coordenação de Aperfeiçoamento de Pessoal de Nível Superior, Grant/Award Number: 001Fundação de Amparo à Pesquisa do Estado de Minas Gerais

Summary

In line with the accomplishment of PQ standards, the search for methodologies to estimate harmonic distortions in large electrical networks, using a small number of meters, emerges as a challenging subject. In this way, this paper proposes a new methodology for HSE in underdetermined power systems monitored with a small number of meters. The HSE approach is modeled as an optimization problem, for which, the solution is achieved using a new strategy, called HA, obtained from the union of the ES algorithm based on CMA with the SADE algorithm. To highlight the approach application, simulations studies are carried out using two transmission systems, and the results enhance the estimation accuracy offered by the HA in comparison to two other HSE methods.

KEYWORDS

Evolutionary algorithms, harmonic distortion, harmonic state estimation, hybrid algorithm, measurement optimization

1 | INTRODUCTION

Power systems face increases in nonlinear loads and inverter-based power sources (eg, photovoltaic and wind power plants), which create concerns for the network operators regarding PQ issues, such as harmonic distortion.[1,2] This phenomenon may be produced by different sources frequently found in both transmission and distribution systems. Therefore, it may be difficult to identify the source of harmonic pollution to apply mitigating strategies.[3,4] Those concerns

List of Symbols and Abbreviations: ANN, artificial neural network; AV, allocation vector; CcV, co-connectivity vector; CM, connection matrix; CKF, cubature Kalman filter; CMA, covariance matrix adaptation; CnV, connectivity vector; DE, differential evolution; ES, evolution strategies; EKF, extended Kalman filter; FV, final vector; GA, genetic algorithm; GPS, global positioning system; HA, hybrid algorithm; HSE, harmonic state estimation; KF, Kalman filter; LP, learning period; LS, least squares; OF, objective function; PMU, phasor measurement unit; PQ, power quality; PSO, particle swarm optimization; RV, redundancy vector; RFM, redundancy-from matrix; RTM, redundancy-to matrix; SADE, self-adaptive differential evolution; SOA, seeker optimization algorithm; SVD, singular value decomposition; THD, total harmonic voltage distortion; WLS, weighted least squares; $\boldsymbol{x}_i$, candidate solution; $\boldsymbol{\sigma}_i$, mutation step; τ and τ', mutation control constants; $\boldsymbol{N}(\mathbf{0},\mathbf{1})$ and $\boldsymbol{N}_i(\mathbf{0},\mathbf{1})$, vectors of random numbers with the normalized Gaussian curve; μ, parents population; λ, descendant population; $\boldsymbol{C}$, covariance matrix; $\boldsymbol{v}_i$, mutant vector; F, mutation factor; $\boldsymbol{u}_i$, trial vector; *rand*(*j*), random number; *CP*, crossover probability; *CPr*, self-adapted *CP*; ***CPm***, stored *CP* values; U^{Mea}, measured voltage; U^{Est}, estimated voltage; I^{Mea}, measured current; I^{Est}, estimated current; Z_k, impedance of branch k.

can be evidenced by the responses of a survey applied by CIGRE and CIRED to transmission and distribution systems operators of 43 countries. The responses provided elected voltage regulation (89% of all respondents), sags and swells (82%), and harmonics (76%) as the most relevant issues to be taken into account. Notably, 79% of the transmission system operator respondents reported having an interest in monitoring harmonics.[5] However, monitoring harmonic distortion in transmission systems can be a challenge because it is impractical and expensive to install PQ monitors on every bus.

To overcome such difficulty, methods for HSE* offer the possibility to estimate harmonic voltages on all buses. In HSE, the state variables are the voltage magnitude and phase angle. Commonly, their values are determined using conventional estimation algorithms, such as LS, WLS, and SVD.[7,9-13] However, the accuracy of these methods can be highly affected by the number of power quality meters and their position on the transmission network. According to Clements[14] and Monticelli,[15] in the context of state estimation of power systems, a system is "observable" when the available measurement set is sufficient to calculate the entire state variables vector of the network uniquely. In this paper, the network observability determines if the state estimation problem can be solved as an LS problem. When the measured variables number is higher or equal to the state variables number, the system is overdetermined or determined and the system is observable. Otherwise, the system is underdetermined, and, hence, it is not completely observable. If this is the case, it is not possible to use conventional algorithms to estimate the state variables.[8]

Faced with those limitations and aiming at the complete estimation of the systems operating conditions, more recent publications presented techniques based on artificial intelligence as an alternative approach to address the drawbacks of the previous methods. In this way, References 16,17 use ES algorithm for HSE, including, in addition to the measurements of harmonic voltage and current phasors, voltage measurements at the fundamental frequency. On the other hand, the methodology of harmonic estimation of Reference 18 uses solely information related to harmonic frequencies. In Reference 19, the SOA is utilized for HSE. In all these studies, the harmonic currents injected into the monitored buses are considered as real-time measurements. However, in practice, PMU with a large number of measurement channels are hardly used in transmission networks.[20] Using a sparse Bayesian learning framework, the authors of Reference 21 proposed a harmonic state estimator to locate the harmonic sources and estimate the voltage distribution. The algorithm assumes that the state variables (injected harmonic currents) present certain probability distributions and that exist few buses producing significant harmonics simultaneously. In the tests, they considered that the maximum number of simultaneous harmonic is 2. Therefore, it is difficult to assess the method in practical cases, because usually there are more than two harmonic sources in power systems.

The papers cited above treat the HSE in the frequency domain. In contrast, Reference 22 introduces an HSE solved in time-domain through the EKF, considering time-varying nonlinear loads, applied in the underdetermined system. In HSE comparative tests using the KF, the EKF, and the SVD, the response of the EKF algorithm was more accurate. However, as a disadvantage, the convergence of this algorithm depends on the determination of the initial parameters. Furthermore, Reference 4 presents an algorithm based on the nodal voltage method and Kron reduction matrix, considering that the global admittance matrix is unknown. The authors of the paper assume that in the nonmonitored part of power systems, there are no harmonic sources. Thus, if this is not the case, the accuracy of this algorithm can be highly affected. In general, References 4,16-19,21 reported good results of harmonic estimation. However, they did not take into account studies on transmission systems with different sizes or if a higher number of nonlinear loads exists.

To overcome the potential limitations of the above-mentioned HSE methods, this paper proposes a novel HA-based approach for HSE in power transmission networks focusing on underdetermined systems. Hybrid algorithms have been successful in several engineering applications, including harmonic component estimation. In Reference 23, the authors proposed an algorithm composed of two fast recursive methods, H∞ filter and CKF, to estimate harmonic amplitudes and phases in separate processes, respectively. With the same purposes, the method of Reference 24 introduced a combination of PSO and GA that optimize KF's parameters. The hybridization proposed here is different from those cited previously; furthermore, we did not find any work in the literature that made this combination, especially when it comes to harmonic state estimation applications. The main contributions of the proposed HSE method are:

1. An HA is developed from the merging of a modern ES algorithm with a SADE algorithm. This combination is based on the convergence speed of the ES algorithm and on the excellent accuracy of SADE for solving real-parameter optimization. Consequently, the resulting algorithm is fast and accurate at determining the values of the state variables.

2. The proposed method needs the meters capable of measuring the harmonic voltage phasor on the bus and the harmonic current phasor in one of the branches connected to the bus, disregarding the existence or not of harmonic sources to perform the measurements. This, in turn, results in a low cost-effective monitoring arrangement.

Simulation studies performed in this paper showed good accuracy in the HSE using HA for tests using two transmission systems, the IEEE-14 bus system and the IEEE-57 bus system. Moreover, in comparative tests, the HA showed better performance than the ES and SOA in terms of estimation accuracy.

This paper has seven sections. Section 2 presents the structure of the proposed methodology. Section 3 describes the proposed HA algorithm. Section 4 explains the observability analysis. Section 5 details the representation of system components and presents the HSE procedures using HA. A critical evaluation of the efficiency of the estimation procedures using HA and comparative studies are the focus of Section 6. Finally, the conclusions are in Section 7.

2 | STRUCTURE OF THE PROPOSED METHODOLOGY

The HA-based HSE proposed in this paper has three modules, as presented in Figure 1. First, module 1 acquires data concerning network topology, parameters of the system components, and measurements of harmonic voltages and current provided by strategically installed PMU. Following this, module 2 executes an observability analysis for checking whether there are unobserved buses and builds up the admittance matrices for the required harmonic orders. Then, module 3 estimates the harmonic voltages by employing the HA for each harmonic order specified in module 2. In the end, the THD can be estimated as a function of the individual harmonic distortions.

3 | HYBRID ALGORITHM

The success of the optimization algorithm depends fundamentally on its adequacy to the optimization problem. In this way, some characteristics of the HSE problem are decisive for the selection of the optimization algorithm, among which stand out:

1. Traditionally, state estimation programs are developed for overdetermined systems of nonlinear equations 8. This paper comprises undetermined systems (systems with more unknowns than equations).
2. The HSE problem has the nodal harmonic current injections as the state variables. Consequently, the optimization problem uses them as candidate solutions (population), establishing an optimization on complex variables.

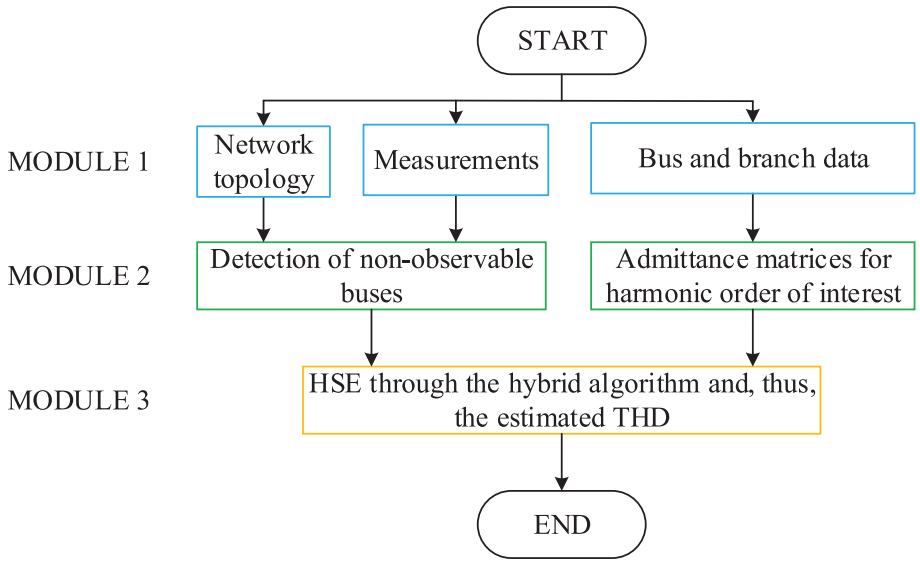

FIGURE 1 Flowchart of the proposed methodology

However, most of the optimization algorithms do not solve complex variables, only real variables. Thus, for using these algorithms, the complex numbers must be represented by a pair of real numbers (either real and imaginary part or magnitude and angle), increasing the search space and convergence time.

3. The injection of harmonic current in buses with low equivalent impedance will have little impact on the objective function. The opposite occurs on nodes with high equivalent impedance. This issue suggests a possible stagnation of algorithms within a local optimum.

Therefore, the requirements of the optimization algorithm are: (a) accuracy in the harmonic voltage estimation of all the buses, with emphasis on those that are not observable, (b) efficiency finding the global optimum quickly, and (c) low risk of getting trapped into a local optimum. With these goals in mind, several algorithms for solving optimization problems over continuous space as, for example, ES algorithm, DE algorithm, SOA, were tested, including their variations. However, they presented problems of stagnation in optimal locations, especially for cases of underdetermined systems, or have a long convergence time, which is significantly increased for large systems. The way to get around this problem was to test the combination of two algorithms. After several attempts, the HA obtained from ES algorithm based on the CMA with the SADE algorithm was reached. Figure 2 gives a flowchart of the proposed HA. The subscripts *abs* and *ang* indicate absolute value and angle, respectively. The variables contained in the flowchart will be defined in the following sections.

Initially, the modern ES algorithm is employed to generate initial solutions. The ES is suited for nonlinear optimization problems. Besides, the authors of References 16,17 also used an ES algorithm for the same purposes of this paper. The difference between the algorithm of the present paper with one employed in these references consists of the CMA. The so-called CMA-ES makes possible the adaptation of mutations to the local shape of the fitness landscape, optimizing the converge procedure. However, evolution strategies are susceptible to getting trapped in a local optimum.[25,26] To solve this issue, the SADE algorithm, a variation of the differential evolution (DE) algorithm, is executed by using the output of the modern ES as the initial population. Only the absolute values of the new individuals are updated, while

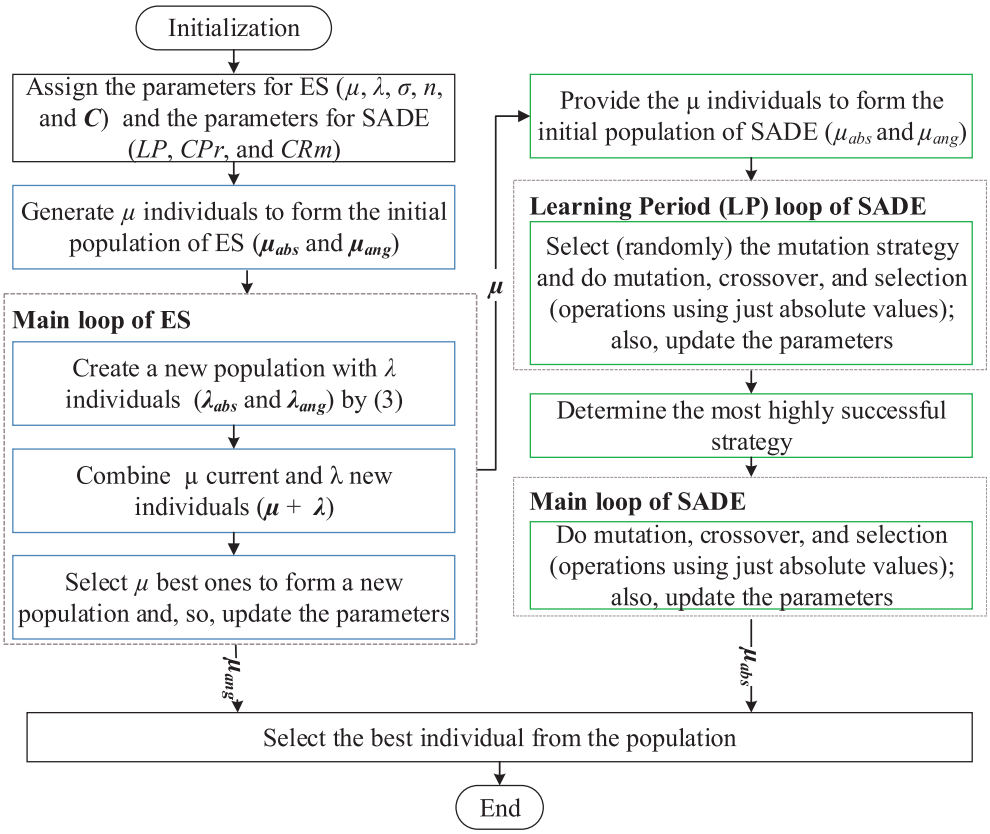

FIGURE 2 Flowchart of the proposed hybrid algorithm. The rectangles with blue edged lines represent ES algorithm steps and the green edged lines, SADE algorithm steps

the respective angles are not changed. The DE algorithm is a search technique for solving optimization problems in continuous space, in elements with real representation, and is known to perform well in nonlinear optimization problems. The main advantage of SADE is the evaluation of different mutation strategies.[27] By combining both algorithms, the HSE has a high success rate, as can be verified in the case studies of Section 6. A sequence of random variables indexed in time with a well-defined correlation structure was considered for simulating the operating conditions of a real system as a stochastic process.

3.1 | Evolution strategies (ES)

The ES is appropriate for optimization problems with real values. The use of a Gaussian mutation operator does not privilege any particular search direction, thus maximizing the search space.[16,17] Two algorithms are embedded in ES: canonical ES and modern ES. Both were implemented in this study in line with.[26]

In the Canonical ES algorithm, each individual from the population is represented by the value of the candidate solution $\boldsymbol{x_i}$ and an adaptive parameter associated with it, called $\boldsymbol{\sigma_i}$. This parameter corresponds to the mutation step. This strategy is known as (x, σ) type. The individual suffers mutation, crossover, and selection, as described in References 16,28. Among these operations, the mutation, defined by Equations (1) and (2), is predominant.

$$\boldsymbol{\sigma}_i^{'} = \boldsymbol{\sigma}_1 e^{\tau N(\mathbf{0},\mathbf{1}) + \tau^{'} \boldsymbol{N}(\mathbf{0},\mathbf{1})} \tag{1}$$

$$\boldsymbol{x_i^{'}} = \boldsymbol{x_1} + \boldsymbol{\sigma}_i \boldsymbol{N_i}(\mathbf{0},\mathbf{1}) \tag{2}$$

where: $\boldsymbol{x_1}$ and $\boldsymbol{\sigma}_1$ are obtained by crossover operation;

τ and $\tau^{'}$ are equal to $\frac{1}{\sqrt{2n}}$ and $\frac{1}{\sqrt{2\sqrt{n}}}$, respectively; n is a constant that controls the mutation variability and should be adequate for each problem;

$\boldsymbol{N}$ (**0,1**) corresponds to a vector of random numbers with the normalized Gaussian curve (with mean 0 and SD 1);

$\boldsymbol{N_i}$ (**0,1**) indicates that the vector of random numbers for each individual is different.

In turn, the crossover is less common and, in general, consists of the arithmetic mean between two or more parents (from $\boldsymbol{x_i}$ and $\boldsymbol{\sigma_i}$). Finally, there exist two selection methods (μ, λ) and $(\mu + \lambda)$. The first considers only the offspring from the population, while the second, utilized by HA, selects the best individuals from the parents and offspring.

The modern ES, an extension of the canonical form of the ES, consists of including a mutation operator, based on a CMA. This strategy is known as $(\boldsymbol{x}, \boldsymbol{\sigma}, \boldsymbol{\theta})$ type. It has the objective of increasing the probability of new generations with the same mutation step and provides a control mechanism for the rate of change of the strategy parameters by maintaining the parameters adjusted without alterations in the case of random selection.[29,30]

As highlighted, the CMA-ES is fundamental in the adaptive process of the mutation. It is divided into two parts: the first, where the covariance matrix $\boldsymbol{C}$ is adapted, and the second, where the mutation step is adjusted.[29] Finally, the process of creating new offspring is originated from a single parent, randomly initialized, and it is obtained as the result of the crossover of several parents. Thus, each offspring is generated according to Equations (3) and (4). The selection consists of assigning the μ best individuals.[25,30]

$$\boldsymbol{x_i^{'}} = \boldsymbol{x_1} + \boldsymbol{w_i}, \tag{3}$$

$$\boldsymbol{w_i} = \boldsymbol{\sigma}_1 \sqrt{\boldsymbol{C}} \boldsymbol{N}(\mathbf{0},\mathbf{1}) \tag{4}$$

3.2 | Differential evolution (DE) algorithm

Similarly to ES, the candidate solutions suffer mutation, crossover, and selection. This procedure occurs so that the current generation is better than or equal to the previous iteration.

The process, according to Reference 28, is indicated using a mutant vector, which is generated by each individual (target vector) of the population ($\boldsymbol{x_i}$), as in Equation (5).

$$\boldsymbol{v_i} = \boldsymbol{x_{r1}} + F(\boldsymbol{x_{r2}} - \boldsymbol{x_{r3}}) \tag{5}$$

where: $\boldsymbol{v_i}$ is the mutant vector;

r_1 , r_2, e r_3 represent three distinct individuals;

F is the mutation factor, a real number defined, usually, between 0 and 2.

To increase diversity within the vector values, the crossover procedure is performed and generates a new vector so-called trial, which is formed according to Equation (6).

$$\boldsymbol{u_i} = \begin{cases} v_{ji} & \text{if } r \text{ and } (j) \leq CPr \\ x_{ji} & \text{if } r \text{ and } (j) > CPr \end{cases} \tag{6}$$

where: $\boldsymbol{v_i}$ is a trial vector;

v_{ji} is the element j of the mutant vector;

x_{ji} is the element j of the target vector;

$rand(j)$ is the random number between 0 and 1;

CPr is the crossover probability.

Finally, the selection operation assigns the best individual between the target vector and the trial vector to set a new population. The best one is chosen by assessing the value of the OF.

The algorithm described above refers to the classic formulation of the DE algorithm. In Reference 31, this method was improved by the insertion of the LP, during which more mutation strategies and a self-adaptive CPr value are tested. This algorithm was called SADE. Its mutation factors vary following a normal distribution. Thus, for the first solutions, these factors tend to create relatively large difference vectors and, consequently, make movements with high magnitudes in search space. On the other hand, with the convergence of the algorithm, their values around the same average may identify the best solutions available. The CPr is obtained through distribution with an average CRm (starting at 0.5) and a SD of 0.1. Thus, different mutation strategies can perform well, using different ranges of crossover probability values. At the end of this period, the most successful mutation strategy (a condition through which the trial vector is replaced in the next generation) will be used to determine the next generations. The value of CRm corresponds to the mean values of CPr stored during the LP.

4 | OBSERVABILITY ANALYSIS

The procedure used in this paper is derived from the studies developed in References 32-35 for the allocation of meters. In this paper, the phasor magnitude and phase angle are considered in the method. Therefore, PMU are needed, and from now on, "meter" refers to PMU. As in Reference 33, in this paper, each meter is capable of measuring the bus i voltage and the current of one branch k. The position of meters is given by the AV, which indicates the buses and branches where the meters are inserted. Hence, the size of the AV is equal to twice the number of branches. Recall that the power system will be observable if all the state variables of voltage (and, hence, current) are directly measured or can be calculated using the measurements available and the network parameter.[33]

The first step consists of analyzing the network topology by obtaining the CM from the inputs ij [where i and j are generic buses in the system, as in Equation (7)]. The sum of the elements of each column corresponds to the branch number that comes out of each bus. Assuming that the lines are transposed, single-phase modeling was performed.

$$cm_{ij} = \begin{cases} 0, & \text{if branch } k \text{ is not connected to buses } i \text{ and } j \\ 1, & \text{if branch } k \text{ is connected to buses } i \text{ and } j \end{cases} \tag{7}$$

Through CM and AV, the treatment given herein refers to a covering problem, which should satisfy the set of restrictions based on Kirchhoff's voltage and current laws:

- Connectivity restriction

This restriction is observed by the connectivity vector (CnV), which determines if the voltage of a particular bus is measured or calculated, as well as if the branch current is measured.

- Redundancy restriction

This restriction is observed by the redundancy vector (RV), which is formulated using redundancy-from matrix and redundancy-to matrix (RFM and RTM, respectively). These matrices evaluate if the voltages between the branches are measured or calculated, indicating if it is possible to obtain the branch currents.

- Co-connectivity restriction

This restriction is analyzed using the co-connectivity vector (CcV), and it is aimed at assuring the possibility of the calculation of the current of a given load or generation, depending on the meters' allocation.

Each restriction described above is a vector whose each position corresponds to the voltage and current state variables. Its values can be obtained through the equations defined by Reference 33. Firstly, each CnV value indicates how many meters monitor the respective variable associated with it. Secondly, RV is a binary vector with a null value for positions regarding voltage variables or current variables that are not observable and a unit value for observable current variables. Finally, the CcV positions in agreement with current variables have a null value, and its remaining positions are filled with values present in CnV and, consequently, have a null value or equal to or greater than 1. Their unification results in the FV. If all the FV elements are greater than or equal to 1, the complete observability of the system is ensured. If not, the voltages or currents not estimated via conventional methods are identified by elements of FV equal to zero.

The focus of this work is the estimation of buses without observability. However, a validation analysis of the estimation method is applied to the system in a condition such that it is fully observable. In this sense, to solve the covering problem and, then, to determine the position of the meters, as in Reference 33, GA was employed. The OF of the GA is given by Equation (8), where $av(i)$ represents each AV position i. In cases where the AV does not meet the restrictions, a high OF value is added. Note that this formulation does not take into account different costs for the possible installation places of meters. As in Reference 33, a calculation of these costs could be introduced with the weighting of AV positions.

$$OF = min \sum_{i=1}^{2 \times n_{branches}} av(i) + \sigma(FV) \tag{8}$$

Considering that FV is obtained by combining the values in the CnV, RV, and CcV, an observable state variable can have, in its position within FV, a value unitary or higher than one. In the last case, this variable has its representation in CnV with a value higher than one, indicating that it has monitoring redundancy. Since CcV is obtained considering elements of CnV, if it is a voltage variable, it is possible that its corresponding position in CcV also has a value superior to one. Thus, we understand that FV also carries the redundancy of this state variable. Therefore, when inserting this calculation to the sum of AV in Equation (8), the solutions that have a redundancy better distributed among all state variables are privileged. Note that the calculation of the SD of $\sigma(FV)$ will have the lowest result in case the monitoring of the variables is more uniform.

5 | ESTIMATION OF HARMONIC DISTORTIONS

Concerning electrical network component models, the transmission lines are represented by their equivalent π model; the transformers by series impedance ($R + j\omega L$); the buses associated with generation points are inserted through the series composition of the stator resistance and *d-axis* sub-transient reactance of the generator ($R_s + jX_d^{\}}$); and the shunt equipment through a shunt admittance ($G + jB$).[36] Notably, in the harmonic frequencies, the loads are inserted considering just their harmonic currents.[16]

Considering that each meter n is designed by one position of AV equal to one, it measures the voltage at bus i and the current at branch k. Then, from the positions with unitary AV values, the sets ΩT and ΩX are obtained. The elements ΩT represent the buses with measured voltages, while those of ΩX, the branches with measured currents. For example, given 2 meters n_1 and n_2 with measurements at buses 2 and 5 and branches 3 and 10, then $\Omega T = \{2, 5\}$ and $\Omega X = \{3, 10\}$. In terms of HSE, the HA has the objective of minimizing the harmonic voltage error of each node and the harmonic current error of the branches indicated by ΩT and ΩX, respectively.

As previously mentioned, this paper characterizes the HSE as an optimization problem. The candidate solutions (that make up the optimization algorithm population) represent the current vector (module and angle) of harmonic injection on the buses of the power system. For each candidate solution, the voltage at the system buses and the branch currents are calculated (estimated) using harmonic power flow. Subsequently, they are evaluated by calculation of the OF, as in Equation (9). Therefore, the OF is given by the sum of squared errors between the measured and estimated voltages, added to the sum of squared errors between the measured and estimated currents, multiplied by the impedance of the branch.

$$OF = min \sum_{i \,\varepsilon\, \Omega T, k \,\varepsilon\, \Omega X} \left|U_i^{Mea} - U_i^{Est}\right|^2 + \left|\left(I_k^{Mea} - I_k^{Est}\right) Z_k\right|^2, \tag{9}$$

where: U_i^{Mea} is the measured voltage at bus i;
U_i^{Est} is the estimated voltage at bus i;
I_k^{Mea} is the measured current at branch k;
I_k^{Est} is the estimated current at branch k;
Z_k is the impedance of branch k.

There is also an evaluation performed over the individual voltage distortions for all buses, where the results with voltages higher than 15% are penalized by Equation (10). This percentage represents an unusual value, much higher than the maximum permitted limits.[37]

$$OF = OF + 100 \times max\left(0, U_i^{Est} - 0.15\right) \tag{10}$$

Over the evolution process, new candidate solutions are generated, and the OF values tend to decrease, and, therefore, the estimated voltages approximate to those indicated by the meters. This process runs until it reaches the stop criteria. In this paper, the number of minimum iterations and error stagnation were used as stop criteria for both algorithms that make up the HA. Due to the involvement of partially observable systems, particular attention is given to harmonic estimation in nonobservable buses, identified by observability analysis.

6 | CASE STUDIES

The performance analysis is implemented over the previously described HA, using the IEEE systems of 14 and 57 buses.[38] The harmonic power flow was implemented in the software MATLAB and validated with the software HarmZs.[39] For the HSE studies, Tables A1 and A3 provide the injected currents, resulting in the values of the voltage distortions of Tables A2 and A4. These tables are given in the Appendix. The proposed HSE approach uses phasor measurements of current and voltage. As with most EEH algorithms, it was assumed that these measurements are synchronized by the GPS. According to Reference 11, synchronization errors with GPS are within 6 μs, which correspond to 0.13 electrical degrees in 60 Hz systems. Therefore, synchronization errors may be negligible. However, bad data (outliers) can originate from problems in the measuring unit or the communication infrastructure. The measurement errors are probably modest in size, but communication errors might produce gross errors.[40] Bad data identification is an important step in the estimation process, but it is outside the scope of this paper. In the studies of this section, bad data are disregarded.

For each of the test systems, the optimal allocation follows the procedures described in Section 4. Then, some meters were removed to establish the condition of an underdetermined system. In terms of parameterization of GA, crossover and mutation probabilities equal to 0.80 and 0.20 were determined, respectively. The parameters of modern

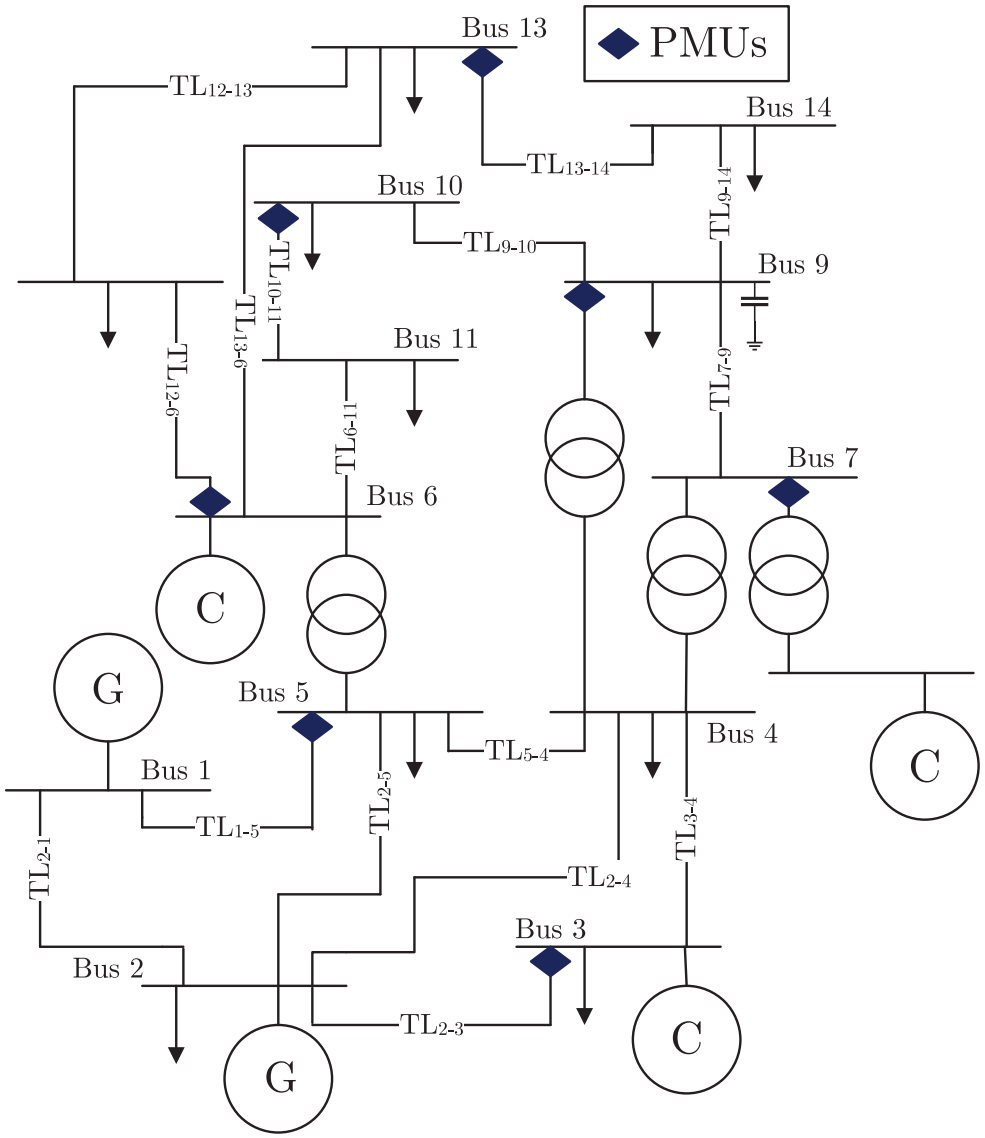

FIGURE 3 Modified IEEE 14-bus system

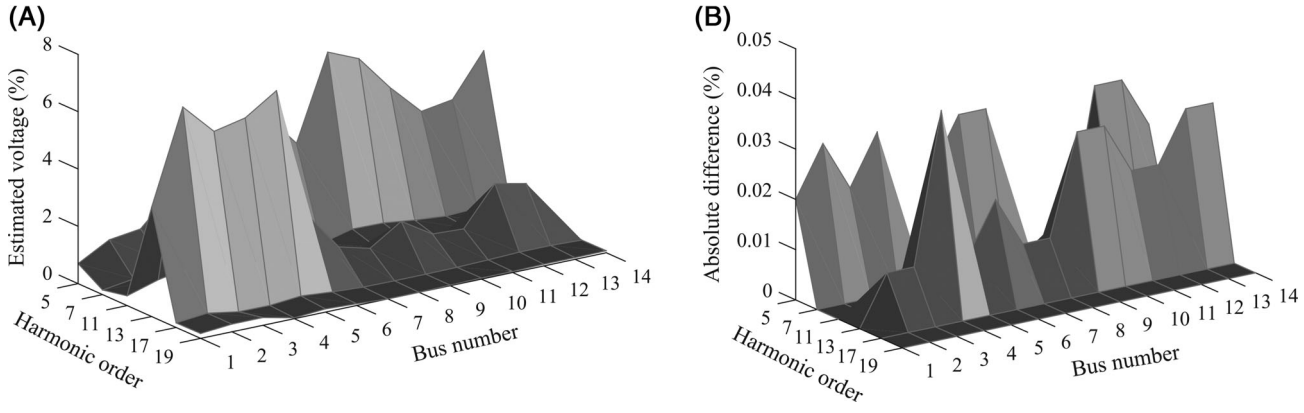

FIGURE 4 Results for the HA (using 7 meters): (a) estimated U_h and (b) absolute estimation errors (%)

ES (CMA-ES) and SADE, which make up the proposed hybrid algorithm to estimate harmonic distortions, followed the adjustment settings defined in References 26,31.

In the modern ES algorithm, the parameter n corresponds to the number of system buses. The parameters σ_{mod} and σ_{ang} are initialized to 0.0001 and 0.0005, respectively, for all individuals of the population. Note that these values are for both test systems and, therefore, suggest that they are also applicable to other transmission systems. In the SADE algorithm, LP was defined empirically, observing which the number of generations would be sufficient to determine the best of the tested four strategies. It is worth noting that the control parameters of SADE are defined randomly over a normal distribution.

The individual number of the population was determined in a guided way for the three algorithms (GA, Modern ES, and SADE). Initially, aiming to generate a great diversity of solutions, it was decided to work with large populations. Subsequently, the number of individuals was varied and assessed empirically, but considering a relationship with the size of the system, that is, the larger the system, the larger the population must be. Similar reasoning could apply to define the population of other transmission systems.

6.1 | IEEE 14-bus electrical system

For the allocation of the meters, the individual number and iterations number of GA was equal to 100 and 300, respectively. In terms of HA, a population of 150 individuals is used; however, for the modern ES, to improve the results, the offspring number was defined as 300. SADE's LP was set at 300 generations. As stop criteria, the error stagnation of the fitness function of modern ES and SADE was determined as 10^{-16} and 10^{-25}, for at least 50 generations, with the minimum number of iterations equal to 1000 and 5000, respectively. The HA was evaluated for each harmonic order 30 times for each situation.

Initially, the condition of a fully observable system was set to test the proposed HSE strategy. Emphasis is placed on the fact that buses 3, 4, 9, 10, 13, and 14 of this system contain nonlinear loads. Figure 3 exhibits one of the allocation results found by the GA. As indicated, 7 meters were allocated. These represent the optimization reached and shows that the voltage measurements were performed on 50% of the buses, and that 35% of harmonic currents of branches were monitored. This value agrees with the results obtained in References 12,33,35,41, which use the same test system employed herein. Figure 4 shows that the HA in the condition of a fully-observable system (7 meters) shows a very good performance concerning the HSE results. The absolute estimation errors are negligible.

For the evaluation of the HA under partially observable conditions, a sequential elimination technique was established, which randomly excludes a meter from time to time. In the following, the results are presented for the errors of the partially observable (with 5 and 3 meters) system situations. The reference values are presented in Table A2 of Appendix. Studies carried out in this paper for monitoring situations using 6 and 4 meters produced similar errors to those when using 5 and 3 meters. Noteworthy here is that the exclusion of meters in different positions across the system results in similar estimation errors, especially when analyzing the THD. For such situations, the results are not provided in this paper.

For 5 meters, 36% of bus harmonic voltages were monitored, as well as 25% of the branches of the harmonic currents. In this way, buses 4, 9, 10, and 11 were not observable, and the HA produced results that were in close agreement with the expected values, as indicated in Figure 5. The situation with 3 meters corresponds to an extreme condition through which only 21% of the buses were effectively monitored regarding harmonic voltages and only 15% of the branches concerning the currents. In this case, buses 1, 4, 5, 6, 9, 10, 11, and 12 were not observable. Again, the HA, as shown in Figure 6, still produced a good performance, with average estimation errors less than 0.25%.

The performance of HA for HSE was also investigated using low values of harmonic distortions. In this case, the injection currents for orders 5, 7, 11, 13, 17, and 19 harmonics correspond to the values in Table A1 of Appendix divided by 10, 1, 2, 12, 2, and 2, respectively. In Figure 7A, the new harmonic voltages are presented. Such voltages are compatible with those established in Reference 37. The estimation results are shown in Figure 7A-C for the cases of 7, 5, and 3 meters. Again, the absolute errors of HSE are negligible for the situation of a determined system with 7 meters. In the case of an underdetermined system, with 5 and 3 meters, the more significant errors were equal to 0.06% (voltage of the 19*th* harmonic in bus 10) and 0.15% (voltage of the 19*th* harmonic in bus 11). Although these errors are more significant, they are still well below the recommended limits. Furthermore, these errors correspond to buses without observability and, in comparison to the other buses, with low levels of distortion for the harmonic orders under analysis.

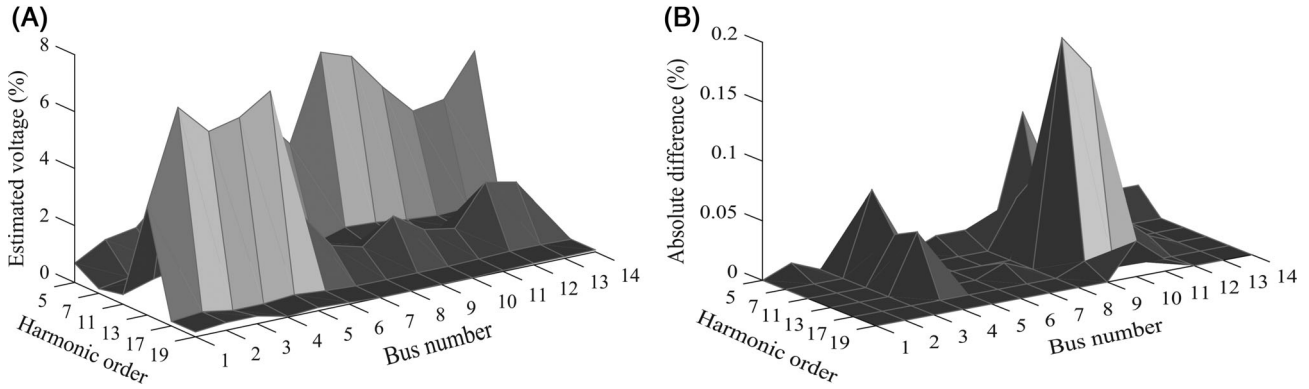

FIGURE 5 Results for the HA (using 5 meters): (a) estimated U_h and (b) absolute estimation errors (%)

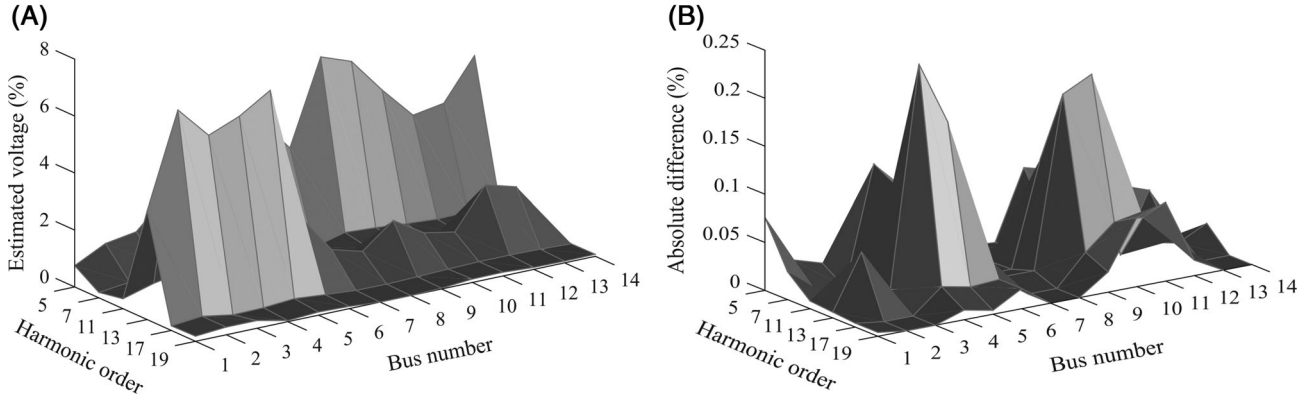

FIGURE 6 Results for the HA (using 3 meters): (a) estimated U_h and (b) absolute estimation errors (%)

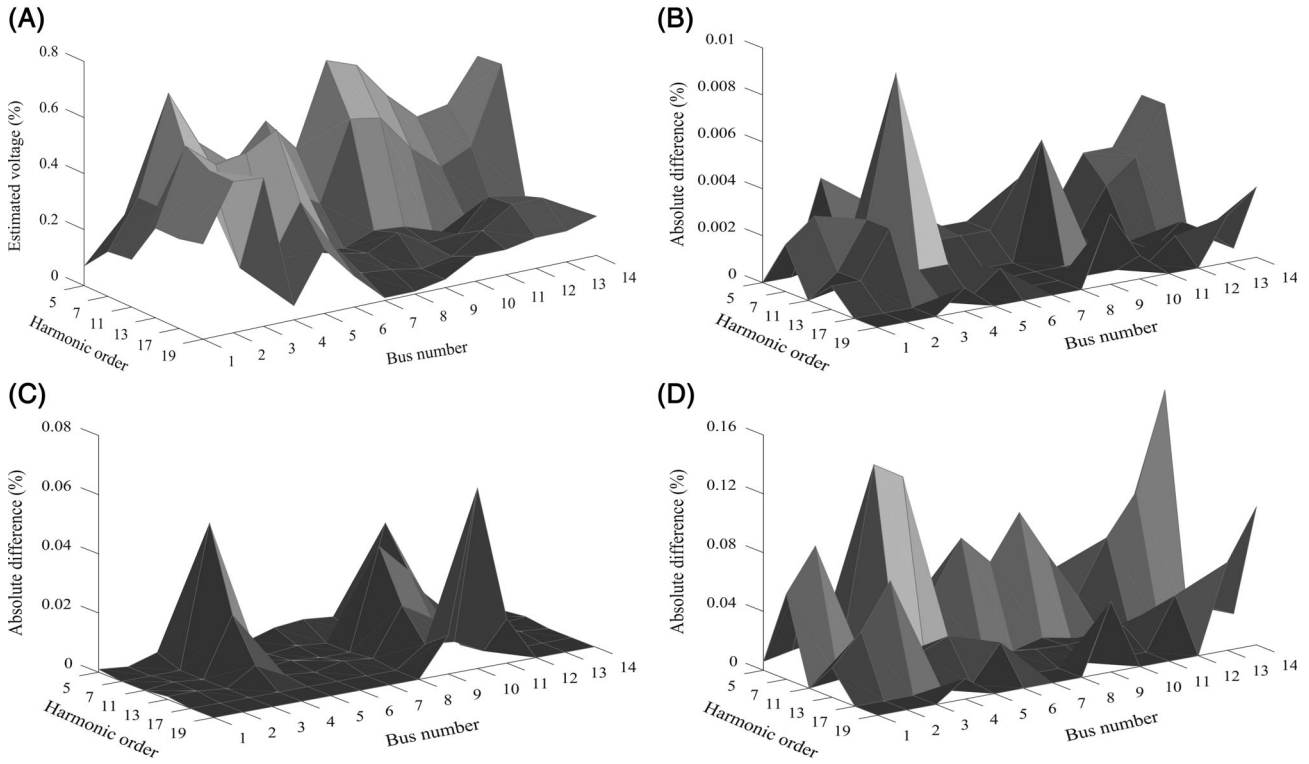

FIGURE 7 HSE results: (a) expected (reference) harmonic voltages; (b) absolute estimation errors (%) error using 7 meters; (c) absolute estimation errors (%) using 5 meters; and (d) absolute estimation errors (%) using 3 meters

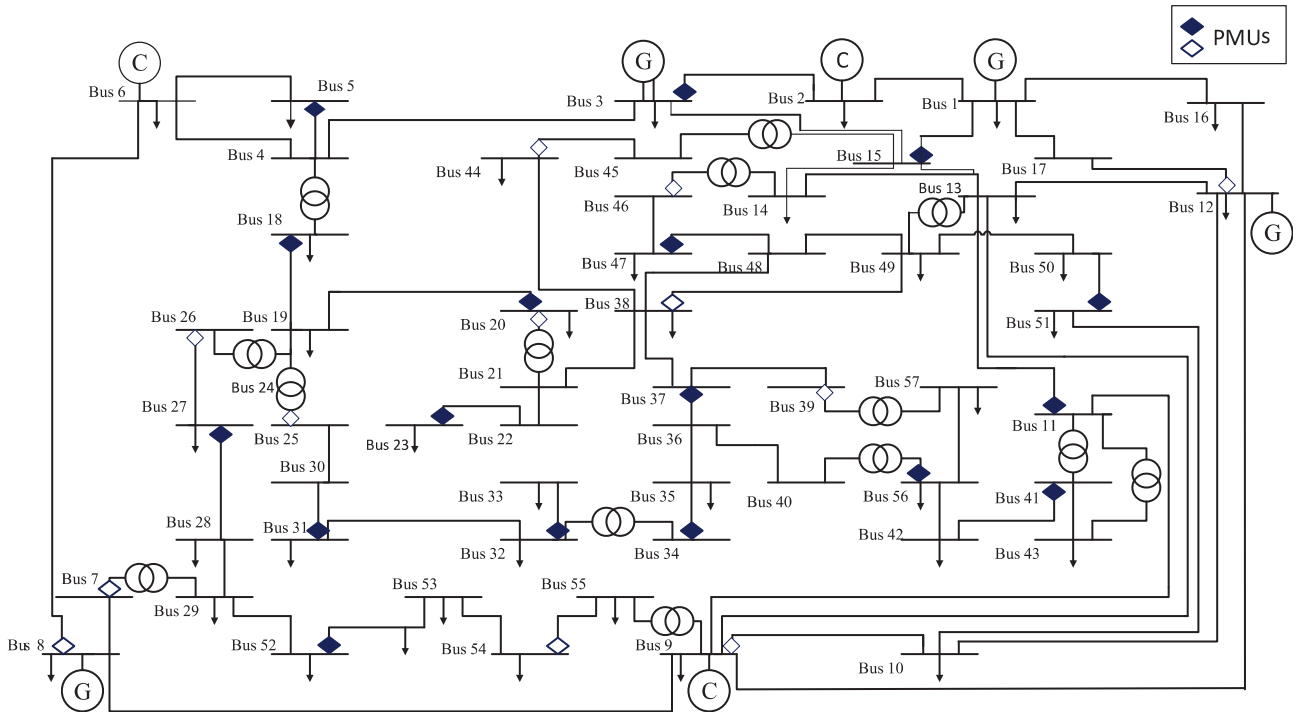

FIGURE 8 Modified IEEE 57-bus system

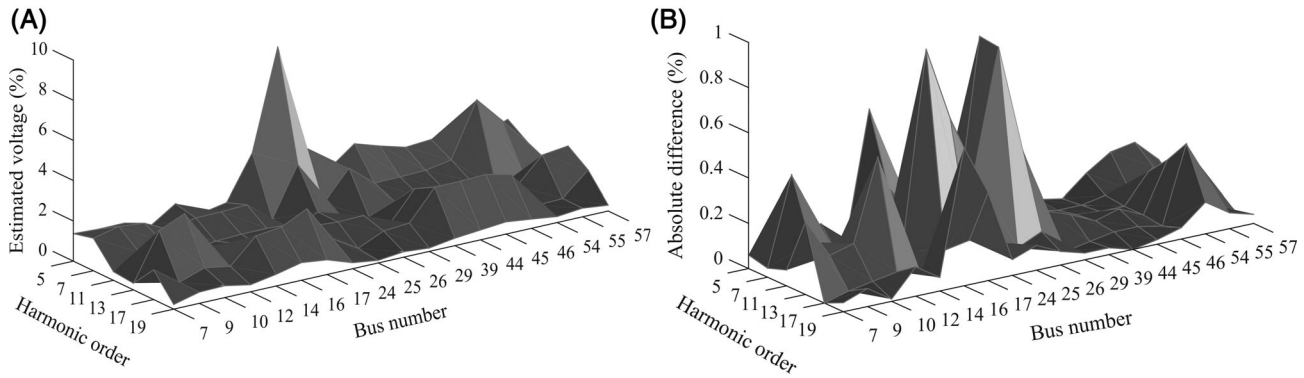

FIGURE 9 Results for the HA (using 19 meters): (a) estimated U_h and (b) absolute estimation errors (%)

6.2 | IEEE 57-bus test system

For full observability, this system requires at least 28 meters, as given in Figure 8. The GA found this result adjusted with a number of individuals equal to 150 and 800 interactions. In this paper, the underdetermined system is to be considered using only the 19 meters (colored ones). This monitoring results in a lack of observability on 18 buses of the system.

Under the requirements related to the 57-bus network, a population with 500 individuals is used for the modern ES algorithm and the SADE. In the case of the modern ES algorithm, the number of offspring is equal to 1000 and the stop criteria were 10^{-16} for the CMA and 10^{-25} for the SADE. SADE's LP was set at 1000 generations. The studies consider a minimum number of 500 iterations for the CMA. The parameters of the algorithms were defined according to References 26,31 or below.

Keeping in mind that this present study is focused on the estimation of buses without observability, only a summary of the HSE results is presented, as given in Figure 9. It is shown that the HA reached errors less than 1%, such as on buses 16 and 25. The average errors were higher at the harmonic components of order 5 and 13. These are, respectively, of 0.31% and 0.15%. Note that, in a general sense, the results of HA are as expected (see Table A4 of Appendix).

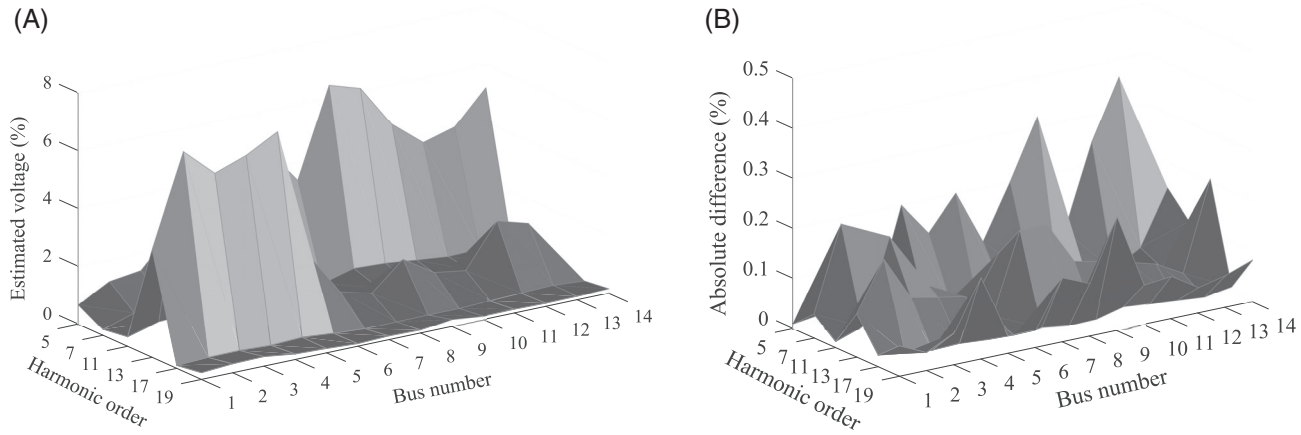

FIGURE 10 Results of the algorithm with canonical ES (using 7 meters): (a) estimated V_h (b) estimation errors

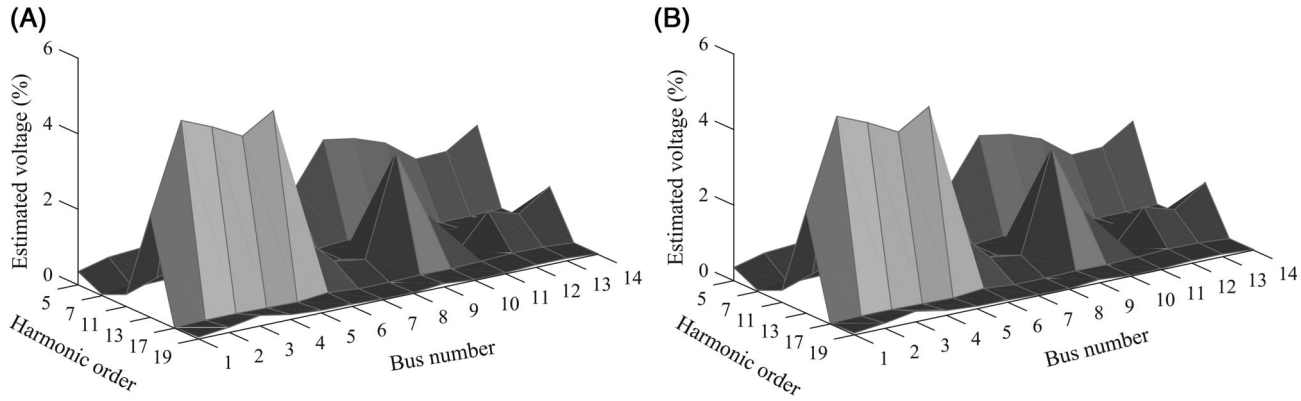

FIGURE 11 Results for the SOA (using 7 meters): (a) estimated V_h and (b) absolute estimation errors (%)

6.3 | Comparisons with other optimization methods applied to HSE

This section compares the proposed HA-based HSE approach with the previously referenced algorithms canonical ES and SOA. The studies employed the same IEEE 14-bus system, used previously in References 16-19.

The canonical ES algorithm was considered in Section 3, and the SOA is given in Reference 19. As for the stop criteria, the error stagnation of the OF was determined at 10^{-25} for at least 50 generations, with the minimum number of iterations equal to 100,000. The other parameters were taken from References 26,31 or are given below.

Canonical ES: number of parents equal to 150, number of offspring equal to 300, $\eta = 2$, $\sigma_{mod} = 0.001$, $\sigma_{ang} = 0.005$ and minimum number of iterations equal to 100 000.

SOA total population equal to 150 individuals divided into three subpopulations, $\mu_{min} = 0.0111$, $\mu_{max} = 0.97$, e $\omega = 0.9$ and the minimum number of iterations equal to 1000.

For comparison purposes, the analyzed cases considered the same number of meters and OF as used for HA in the previous section. The average of the absolute errors of THD of the buses associated with each evolutionary algorithm will be presented as a criterion for the comparative performance analysis.

- 7 meters (determined system)

For the canonical ES algorithm, the results were inaccurate for the 30 simulations performed. The errors were higher than 0.3% for the 5*th* harmonic order at the buses 10 and 13 as shown in Figure 10.

As for the SOA algorithm, harmonic voltage absolute errors of up to 4% were found, as evident in Figure 11. As such, this algorithm was not considered for systems under underdetermined conditions.

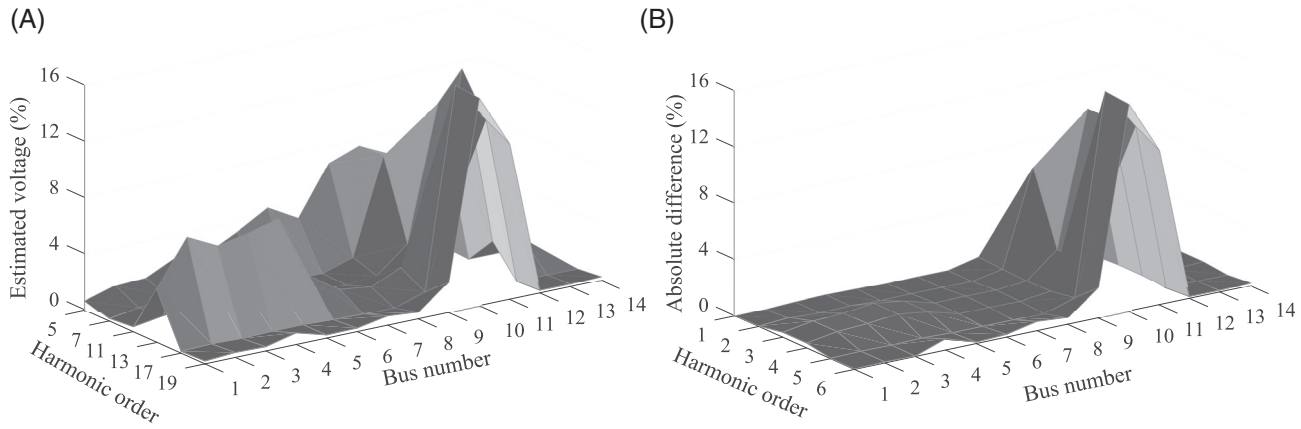

FIGURE 12 Results for the canonical ES algorithm (using 5 meters): (a) estimated V_h and (b) absolute estimation errors (%)

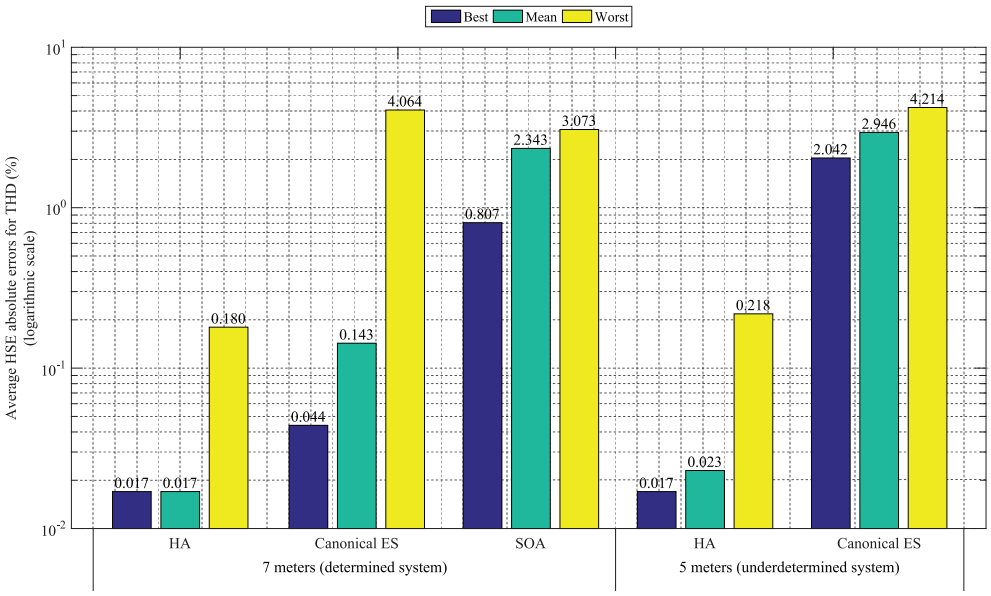

FIGURE 13 Comparative analysis for total harmonic distortion for the presented algorithms

- 5 meters

As given in Figure 12, the canonical ES algorithm presented harmonic voltage absolute estimation errors higher than 14%. Therefore, it is recognized that this algorithm found difficulties in reaching the expected solution (see Table A2 of Appendix).

Figure 13 demonstrates the relationship between the performances of the procedures using the average HSE absolute errors related to the total distortions of the 14-bus network. In the case of using 7 meters, one notes that the SOA algorithm presented the highest error, while the canonical ES was shown as chaotic only in the worst situation. The HA presented contemptible errors for the best, mean, and worst situation. When 5 meters were used, the canonical ES algorithm did not present a good performance for the three analyzed situations, while the HA showed to be efficient even with this reduced number of meters.

In summary, the results have shown that:

- The canonical ES algorithm has demonstrated good performance with determined systems. On the other hand, if the system is underdetermined, for instance, with 5 meters, the approach has shown to be quite inadequate;
- The SOA did not lead to an adequate performance even when an observable system condition was considered;

- Finally, the HA showed to be the most efficient as fewer deviations were encountered among the best, the worst, and average results found. Besides, the proposed methodology has shown good accuracy for the harmonic distortions for the two test systems used.

7 | CONCLUSIONS

This paper presented a new approach based on HA for HSE in undetermined transmission power systems, with a reduced number of meters. This way, an observability analysis identifies the nonobservable portion of the system. The proposed HA takes advantage of modern ES and SADE in terms of (a) rapid upgrading of the initial population and (b) performance in the search for a global solution. With this approach, the harmonic voltage estimation in undetermined systems has been very effective, so that it can be used to minimize harmonic monitoring costs in transmission systems.

The proposed approach showed better performance than the canonical ES algorithm[26] and SOA.[19] Therefore, it is demonstrated that the HA is much superior to the other two investigated algorithms, suggesting significant gains for HA in terms of estimation accuracy in the analyzed cases. Besides, when tested with a complex network, such as the IEEE 57-bus system, the proposed method presented estimation errors smaller than 1%. Noteworthy is that, this case resulted in a more complex optimization problem to solve, proving that the HA is robust and credible for real applications. Future works could also study the application of HA-based optimization approaches for solving the HSE problem in distribution systems.

ACKNOWLEDGEMENTS

This study was financed in part by the Foundation for Research of the State of Minas Gerais (FAPEMIG) and Coordenação de Aperfeiçoamento de Pessoal de Nível Superior - Brasil (CAPES) - Finance Code 001.

ENDNOTE

* The term "harmonic state estimation" refers to the identification of the static state of the harmonic voltages (magnitude and phase) in all network buses[6-8]

PEER REVIEW

The peer review history for this article is available at https://publons.com/publon/10.1002/2050-7038.12763.

DATA AVAILABILITY STATEMENT

The data that supports the findings of the case studies performed in this paper are available in the cited references.

ORCID

Gustavo G. Santos https://orcid.org/0000-0002-0231-1772
Thales L. Oliveira https://orcid.org/0000-0001-7189-5110

REFERENCES

1. Luo A, Chen Y, Shuai Z, et al. Large-scale photovoltaic plant harmonic transmission model and analysis on resonance characteristics. *IET Power Electron*. 2015;8(4):565-573.
2. Mishra A, Tripathi PM, Chatterjee K. A review of harmonic elimination techniques in grid connected doubly fed induction generator based wind energy system. *Renewable Sustainable Energy Rev*. 2018;89:1-15.
3. Garca H, Segundo J, Madrigal M. Harmonic analysis of power systems including thyristor-controlled series capacitor (TCSC) and its interaction with the transmission line. *Electr Power Syst Res*. 2014;106:151-159.
4. Bečirović V, Pavić I, Filipović-Grčić B. Sensitivity analysis of method for harmonic state estimation in the power system. *Electr Power Syst Res*. 2018;154:515-527.
5. Milanovic JV, Meyer J, Ball RF, et al. International industry practice on power-quality monitoring. *IEEE Trans. Power Delivery*. 2014;29 (2):934-941.
6. Schweppe FC. Power system static-state estimation, Part III: implementation. *IEEE Trans. Power Appar. Syst.* 1970 Jan;PAS-89(1): 130-135.
7. Heydt GT. Identification of harmonic sources by a state estimation technique. *IEEE Trans. Power Delivery*. 1989;4(1):569-576.
8. Monticelli A. *State Estimation in Electric Power Systems*. Boston, MA: Springer US; 1999.

9. Najjar MY, Heydt GT. A hybrid nonlinear-least squares estimation of harmonic signal levels in power systems. *IEEE Trans Power Delivery*. 1991;6(1):282-288.
10. Du ZP, Arrillaga J, Watson N. Continuous harmonic state estimation of power systems. *IEE Proc - Gener Transm Distrib*. 1996;143(4):329-336.
11. Kanao N, Yamashita M, Yanagida H, Mizukami M, Hayashi Y, Matsuki J. Power system harmonic analysis using state-estimation method for Japanese field data. *IEEE Trans Power Delivery*. 2005;20(2):970-977.
12. Rad MS, Mokhtari H, Karimi H. An optimal measurement placement method for power system harmonic state estimation. Paper presented at: 2012 International Conference and Exposition on Electrical and Power Engineering; October 25-27, 2012; Iasi, Romania:271-275.
13. Rakpenthai C, Uatrongjit S, Watson NR, Premrudeepreechacharn S. On Harmonic State Estimation of Power System With Uncertain Network Parameters. *IEEE Transactions on Power Systems*. 2013;28(4):4829–4838. http://dx.doi.org/10.1109/tpwrs.2013.2273943.
14. Clements KA. Observability methods and optimal meter placement. *Int J Electr Power Energy Syst*. 1990;12(2):88-93.
15. Monticelli A. Electric power system state estimation. *Proc IEEE*. 2000;88(2):262-282.
16. Arruda EF, Kagan N, Ribeiro PF. Harmonic distortion state estimation using an evolutionary strategy. *IEEE Trans Power Delivery*. 2010; 25(2):831-842.
17. Arruda EF, Kagan N, Ribeiro PF. Three-phase harmonic distortion state estimation algorithm based on evolutionary strategies. *Electr Power Syst Res*. 2010;80(9):1024-1032.
18. do Nascimento Sepulchro W, Encarnação LF, Brunoro M. Harmonic State and Power Flow Estimation in Distribution Systems Using Evolutionary Strategy. *Journal of Control, Automation and Electrical Systems*. 2014;25(3):358–367. http://dx.doi.org/10.1007/s40313-014-0110-1.
19. Ketabi A, Sheibani MR, Nosratabadi SM. Power quality meters placement using seeker optimization algorithm for harmonic state estimation. *Int J Electr Power Energy Syst*. 2012;43(1):141-149.
20. Miljanić Z, Djurović I, Vujošević I. Optimal placement of PMUs with limited number of channels. *Electr Power Syst Res*. 2012 sep;90:93-98.
21. Yuan Y, Zhou W, Zhang HT, Ping Z, Ardakanian O. Sparse Bayesian harmonic state estimation. Paper presented at: 2018 IEEE International Conference on Communications, Control, and Computing Technologies for Smart Grids (SmartGridComm); October 29-31, 2018; Aalborg, Denmark:IEEE.
22. Cisneros-Magaña R, Medina A, Anaya-Lara O. Time-domain harmonic state estimation of nonlinear load power systems with underdetermined condition based on the extended Kalman filter. *Int Trans Electr Energy Syst*. 2016;27(2):e2242.
23. Enayati J, Moravej Z. Real-time harmonic estimation using a novel hybrid technique for embedded system implementation. *International Transactions on Electrical Energy Systems*. 2017;27(12):e2428. http://dx.doi.org/10.1002/etep.2428.
24. Xi Y, Tang X, Li Z, et al. Harmonic estimation in power systems using an optimised adaptive Kalman filter based on PSO-GA. *IET Gener Transm Distrib*. 2019;13(17):3968-3979.
25. Beyer HG, Schwefel HP. Evolution strategies – A comprehensive introduction. *Nat Comput*. 2002;1(1):3-52.
26. Beyer HG. Evolution strategies. *Scholarpedia*. 2007;2(8):1965.
27. Mohamed AW, Sabry HZ, Khorshid M. An alternative differential evolution algorithm for global optimization. *J Adv Res*. 2012;3(2):149-165.
28. Soliman SAH, Mantawy AAH. *Modern Optimization Techniques with Applications in Electric Power Systems*. 1st ed. New York: Springer-Verlag; 2010.
29. Hansen N, Ostermeier A. Adapting arbitrary normal mutation distributions in evolution strategies: the covariance matrix adaptation. Paper presented at: Proceedings of IEEE International Conference on Evolutionary Computation; May 20-22, 1996; Nagoya, Japan: 312-317.
30. Bäck T, Foussette C, Krause P. *Contemporary Evolution Strategies*. 1st ed. Berlin, Heidelberg: Springer-Verlag; 2013.
31. Qin AK, Huang VL, Suganthan PN. Differential evolution algorithm with strategy adaptation for global numerical optimization. *IEEE Trans Evol Comput*. 2009;13(2):398-417.
32. Reis DCS, Villela PRC, Duque CA, Ribeiro PF. Transmission systems power quality monitors allocation. Paper presented at: 2008 IEEE Power and Energy Society General Meeting - Conversion and Delivery of Electrical Energy in the 21st Century; July 20-24, 2008; Pittsburgh, PA: 1-7.
33. Almeida CFM, Kagan N. Harmonic state estimation through optimal monitoring systems. *IEEE Trans Smart Grid*. 2013;4(1):467-478.
34. Eldery MA, El-Saadany F, Salama MMA. Optimum number and location of power quality monitors. Paper presented at: 2004 11th International Conference on Harmonics and Quality of Power (IEEE Cat. No.04EX951); September 12-15, 2004; Lake Placid, NY:50-57.
35. Almeida CFM, Kagan N, Souza TP, et al. Locating power quality meters in order to perform harmonic state estimation. Paper presented at: 2012 IEEE 15th International Conference on Harmonics and Quality of Power; June 17-20, 2012; Hong Kong, China: 662-667.
36. Arrillaga J, Arnold CP. *Computer Analysis of Power Systems*. Chichester: Wiley; 1990.
37. IEEE Recommended Practice and Requirements for Harmonic Control in Electric Power Systems. IEEE Std 519-2014 (Revision of IEEE Std 519-1992); 2014:1-29.
38. Power Systems Test Case Archive; Online; 10/14/2020. https://labs.ece.uw.edu/pstca/.
39. CEPEL. HarmZs (version 3.0). Academic license; 2016.
40. Phadke A. *Synchronized Phasor Measurements and their Applications*. New York: Springer; 2008.
41. Liao H. Power system harmonic state estimation and observability analysis via sparsity maximization. *IEEE Trans Power Syst*. 2007;22(1):15-23.

How to cite this article: Santos GG, Oliveira TL, Oliveira JC, Vieira JCM. A hybrid method for harmonic state estimation in partially observable systems. *Int Trans Electr Energ Syst*. 2021;31:e12763. https://doi.org/10.1002/2050-7038.12763

APPENDIX A.

The injected harmonic currents and the harmonic voltages resulting in harmonic flow, for the IEEE 14-bus harmonic test system, are present on Tables A1 and A2. The harmonic voltage data are given as reference values for the HSE studies in Subsections 6.1 and 6.3.

TABLE A1 Injected harmonic currents (module in A and angle in degrees)

Bus		I_{5h}	I_{7h}	I_{11h}	I_{13h}	I_{17h}	I_{19h}
3	Module	12.3580	6.1790	2.4459	4.9561	1.2229	1.2229
	Angle	20.2400	237.1500	347.5900	149.7000	149.7000	144.1700
4	Module	12.3580	6.1790	2.4459	4.9561	1.2229	1.2229
	Angle	184.3000	232.6200	47.1800	153.8500	153.8500	123.1400
9	Module	26.0677	13.1947	5.1492	10.2983	2.5746	2.5746
	Angle	82.7300	113.6400	247.1300	186.0900	186.0900	79.1700
10	Module	9.0110	4.5055	1.9309	3.5400	0.9655	0.9655
	Angle	142.2400	313.0900	197.1400	241.6100	241.6100	274.2300
13	Module	10.2983	5.1492	1.9309	4.1837	0.9655	0.9655
	Angle	32.0300	85.0000	184.5800	303.4400	303.4400	28.2300
14	Module	14.1602	7.0801	2.8964	5.7928	1.2873	1.2873
	Angle	199.8200	47.9900	126.3200	107.4700	107.4700	187.7100

TABLE A2 Results from the voltage distortions (in %) of reference (IEEE 14-bus)

Bus	U_5	U_7	U_{11}	U_{13}	U_{17}	U_{19}	THD
1	0.6735	0.1591	0.3443	3.8127	0.1604	0.1717	3.8973
2	1.2704	0.3263	0.6628	7.0683	0.2691	0.2723	7.2296
3	1.4636	0.6777	0.8702	5.9942	0.0865	0.2657	6.2743
4	2.5217	0.4849	0.7478	6.2013	0.0850	0.0260	6.7541
5	2.2520	0.3905	0.7241	6.9505	0.1802	0.1150	7.3555
6	3.2560	0.1621	0.1807	2.4080	0.0939	0.0568	4.0584
7	4.4675	0.2378	0.1268	1.0665	0.0320	0.0042	4.6011
8	3.2682	0.1739	0.0928	0.7802	0.0234	0.0031	3.3659
9	6.2419	0.4518	0.1800	1.4587	0.0173	0.0135	6.4286
10	5.7778	0.4304	0.1535	0.7784	0.0267	0.0459	5.8482
11	4.5389	0.2980	0.0355	0.7881	0.0582	0.0452	4.6172
12	3.5017	0.2103	0.1365	2.1308	0.0959	0.0560	4.1082
13	3.6936	0.2631	0.1142	1.9136	0.0974	0.0566	4.1712
14	5.1601	0.5289	0.1829	0.2744	0.0641	0.0688	5.1985

The injected harmonic currents and the harmonic voltages resulting in harmonic flow, for the IEEE 57-bus harmonic test system, are present on Tables A3 and A4. The harmonic voltage data are given as reference values for the HSE studies in Subsection 6.2.

TABLE A3 Injected harmonic currents (module in pu - 100 MVA and angle in degrees)

white Bus		I_{5h}	I_{7h}	I_{11h}	I_{13h}	I_{17h}	I_{19h}
2	Module	0.02663	0.01856	0.01657	0.017620	0.00286	0.00178
	Angle	333.4922	178.6782	315.8388	76.7657	41.1845	44.7536
3	Module	0.00904	0.00725	0.00732	0.004418	0.00228	0.00300
	Angle	295.3677	14.3451	347.8279	319.6686	229.9586	3.9435
9	Module	0.01623	0.03692	0.01529	0.006231	0.00056	0.00003
	Angle	68.0662	176.8333	221.9288	44.1994	47.8914	113.1051
13	Module	0.00168	0.00500	0.00074	0.000361	0.00117	0.00071
	Angle	150.3509	39.7610	198.9880	40.0610	84.9681	49.9155
16	Module	0.01612	0.01434	0.00068	0.003809	0.00120	0.00125
	Angle	350.6235	85.6423	39.0875	288.0105	16.1325	345.5843
17	Module	0.01729	0.01378	0.00547	0.008901	0.00169	0.00149
	Angle	91.0949	70.5460	177.3844	255.9183	355.5427	120.4631
27	Module	0.00123	0.00008	0.00007	0.000333	0.00006	0.00029
	Angle	171.5091	39.5990	156.7554	324.6763	203.7002	263.0317
29	Module	0.00646	0.00321	0.00272	0.003292	0.00045	0.00014
	Angle	189.0436	122.8050	305.7850	67.0434	75.1482	190.9551
30	Module	0.00001	0.00043	0.00047	0.000604	0.00014	0.00023
	Angle	210.8427	275.8792	62.8685	181.1213	137.7630	351.7914
31	Module	0.00646	0.00321	0.00272	0.003292	0.00045	0.00014
	Angle	189.0436	122.8050	305.7850	67.0434	75.1482	190.9551
32	Module	0.00008	0.00046	0.00034	0.000185	0.00004	0.00010
	Angle	343.6295	232.5182	174.7150	157.7455	67.0975	159.5283
35	Module	0.00224	0.00082	0.00072	0.000336	0.00009	0.00038
	Angle	24.0024	70.5105	350.9215	207.0326	209.9569	342.0078
41	Module	0.00000	0.00200	0.00096	0.000605	0.00023	0.00019
	Angle	162.7405	9.6335	153.1031	38.0899	15.5201	200.2040
42	Module	0.00260	0.00090	0.00128	0.001254	0.00030	0.00052
	Angle	280.5787	178.1497	274.1426	240.1361	352.1204	42.1455
43	Module	0.00053	0.00011	0.00046	0.000395	0.00001	0.00004
	Angle	147.4668	225.6512	330.8771	149.4546	256.1401	349.5149
47	Module	0.00110	0.01049	0.00570	0.003026	0.00135	0.00079
	Angle	273.2744	212.1987	220.1652	303.5414	164.5156	317.8043
49	Module	0.00471	0.00605	0.00229	0.003287	0.00062	0.00127
	Angle	31.1713	359.6174	261.9292	201.0264	51.4167	301.5493
50	Module	0.00413	0.00270	0.00156	0.002875	0.00114	0.00142
	Angle	75.9091	182.4306	153.0179	86.2920	272.7084	285.0883

TABLE A4 Results from the voltage distortions (in %) of reference (IEEE 57-bus)

Bus	U_5	U_7	U_{11}	U_{13}	U_{17}	U_{19}	THD
7	1.3054	1.5824	0.3531	0.0049	1.4833	0.1952	2.5634
9	1.4192	2.3440	1.2810	2.5207	0.5448	0.4792	4.0037
10	1.4351	1.8515	1.3893	3.4099	0.9652	0.5763	4.5066
12	0.9998	1.1883	0.7928	1.8212	0.7155	0.2150	2.6297
14	1.6929	1.4526	0.8730	1.2726	2.0576	0.6379	3.4638
16	1.5362	1.7831	0.8729	1.7311	2.0608	0.2733	3.6905
17	1.4658	1.7068	0.9266	0.8695	2.9386	1.1197	4.0701
24	3.5254	0.4765	0.4315	0.7985	0.9113	0.2342	3.7900
25	8.2481	3.0529	0.1799	0.1734	0.1970	0.0209	8.8007
26	3.3100	0.6527	0.3857	0.6929	0.7233	0.2129	3.5468
29	1.5072	2.1984	0.2122	0.2273	0.9341	0.1362	2.8447
39	2.5492	1.1488	0.7368	1.7683	2.3956	0.3483	4.1651
44	2.2369	1.1849	0.7494	1.3580	2.3906	0.4868	3.8426
45	1.9313	1.2280	0.7428	0.6980	2.4319	0.6347	3.5487
46	1.9189	1.4386	0.8596	1.5211	2.2163	0.5075	3.7382
53	2.1110	5.4026	0.7650	0.6543	0.3241	0.0666	5.8964
54	1.8333	4.1547	0.0737	0.6221	0.0249	0.1541	4.5869
57	2.0701	1.4754	0.9297	2.3424	1.5302	0.2421	3.9004